

Bulk sensitive photo emission spectroscopy of C_{1b} compounds.

Gerhard H. Fecher, Andrei Gloskowski, Kristian Kroth,
Joachim Barth, Benjamin Balke, and Claudia Felser
Institut für Anorganische Chemie und Analytische Chemie,
Johannes Gutenberg – Universität, 55099 Mainz, Germany

Franz Schäfers, Marcel Mertin, and Wolfgang Eberhardt
BESSY GmbH, Albert-Einstein-Strasse 15, 12489 Berlin, Germany

Sven Mahl, and Oliver Scha
SPECS GmbH, Voltastraße 5, 13355 Berlin, Germany

(Dated: March 23, 2022)

Abstract

This work reports about bulk-sensitive, high energy photoelectron spectroscopy from the valence band of C_{1b} excited by photons from 1.2 to 5 keV energy. The high energy photoelectron spectra were taken at the KMC-1 high energy beam line of BESSY II employing the recently developed Phoibos 225 HV analyser. The measurements show a good agreement to calculations of the electronic structure using the LDA scheme. It is shown that the high energy spectra reveal the bulk electronic structure better compared to low energy XPS spectra.

PACS numbers: 79.60.-i, 79.60.Bm, 71.20.Lp, 71.20.Nr

Keywords: Photoemission, Electronic structure, Intermetallics, Semiconductor

Electronic address: fecher@uni-mainz.de

I. INTRODUCTION

Photo emission spectroscopy is the method of choice to study the occupied electronic structure of materials. Low kinetic energies result in a low electron mean free path being only 5.3 Å at kinetic energies of 100 eV or 26 Å at 1.2 keV (all values calculated for CoTeSb using the Tamura-Powell-Penn (TPP-2M) equations [1]). A depth of less than one cubic cell will contribute to the observed intensity if using VUV (< 40 eV) or XUV (< 120 eV) light for excitation. The situation becomes much better at high energies. In the hard X-ray region of about 5 keV one will reach a high bulk sensitivity with an escape depth being larger than 84 Å (corresponding to 15 cubic cells). Lindau et al [2] demonstrated in 1974 the possibility of high energy photo emission with energies up to 8 keV, however, no further attention was devoted to such experiments for many years. High energy photo emission (at about 15 keV excitation energy) was also performed as early as 1989 [3] using a ^{57}Co Mössbauer source for excitation, however, with very low resolution only. Nowadays, high energy excitation and analysis of the electrons become easily feasible due to the development of high intense sources (insertion devices at synchrotron facilities) and multi-channel electron detection. Thus, high energy X-ray photo emission spectroscopy (HXPES) was recently introduced by several groups [4, 5, 6, 7, 8, 9] as a bulk sensitive probe of the electronic structure in complex materials. In the present work, excitation energies of $h\nu = 1.2 :: 5$ keV were used to study the density of states of CoTeSb.

CoTeSb crystallises in the $C1_b$ structure. This structure type is often observed in ternary (XYZ) transition metal (X, Y) intermetallics with a main group element (Z). It is based on a face-centered cubic lattice (space group $F\bar{4}3m$) similar to the binary zinc-blende type semiconductors. Many of the $C1_b$ compounds belong to the class of half-metallic ferromagnets [10]. CoTeSb carries no magnetic moment according to the Slater-Pauling rule because it has overall 18 valence electrons. Most of the $C1_b$ compounds with 18 valence electrons are found to be semiconducting [11].

II. EXPERIMENTAL AND CALCULATIONAL DETAILS

CoTeSb samples have been prepared by arc melting of stoichiometric amounts of the constituents in an argon atmosphere at 10^{-4} mbar. Care has been taken to avoid oxygen

contamination. This was ensured by evaporating Ti inside of the vacuum chamber before melting the compound as well as by additional purification of the process gas. After cooling of the resulting polycrystalline ingots, they were annealed in an evacuated quartz tube for 21 days. This procedure resulted in samples exhibiting the $C1_b$ structure, which was verified by X-ray powder diffraction (XRD). Magneto-structural investigations on Fe substituted samples ($CoTi_{1-x}Fe_xSb$) were carried out using ^{57}Fe Mössbauer spectroscopy. The magnetic properties of Fe doped samples were investigated by a superconducting quantum interference device. The resistivity of the samples was measured by a 4-point probe. Further details and results of the structural and magnetic properties are reported elsewhere [12].

An ESCALAB MKII-HV (VG) for kinetic energies up to 15 keV [3, 13] has been used here to take valence band spectra at an excitation energy of 1.253 keV (Mg K with a line width of $\Delta E = 0.15$ eV) for comparison. For this purpose, the slits and pass energy have been set for a resolution of 200 meV. The energy is calibrated at the Au $4f_{7/2}$ emission line. X-ray photoelectron spectroscopy (XPS) was also used to verify the composition and to check the cleanliness of the samples. After removal of the native oxide from the polished surfaces by Ar^+ ion bombardment, no impurities were detected with XPS.

Details of the electronic structure have been explored experimentally by means of high energy X-ray photo emission spectroscopy. The measurements have been performed at the KMC-1 beam line of the storage ring BESSY II (Berlin, Germany). The photons are produced by means of a bending magnet. The photon beam is focused by a toroidal mirror and monochromatized by a double-crystal monochromator. Three different crystal pairs – that are InSb(111), Si(111), and Si(422) – can be employed for photon energies up to 15 keV with starting energies of 1.674, 1.997, and 5.639 keV, respectively. The crystals can be changed in situ. The acceptance of the toroidal Si/Pt mirror is (6 ± 0.5) mrad². The resulting spot size of the beam is (0.4×0.6) mm² at the focus being located about 35 m behind the source. The complete beam line is operated under oil-free UHV conditions ($< 5 \times 10^{-8}$ mbar at last valve). The characteristics of the beam line flux and resolution using Si(111) and Si(422) crystals – are displayed in Figure 1 (a) and (b).

A selector analyser, a recently developed hemispherical spectrometer with 225 mm radius has been used (Phoibos 225 HV). The analyser is designed for high resolution spectroscopy at kinetic energies up to 15 keV. For the present study, a 2D-CCD detector has been employed for detection of the electrons. The analyser is prepared for parallel 2D (energy and

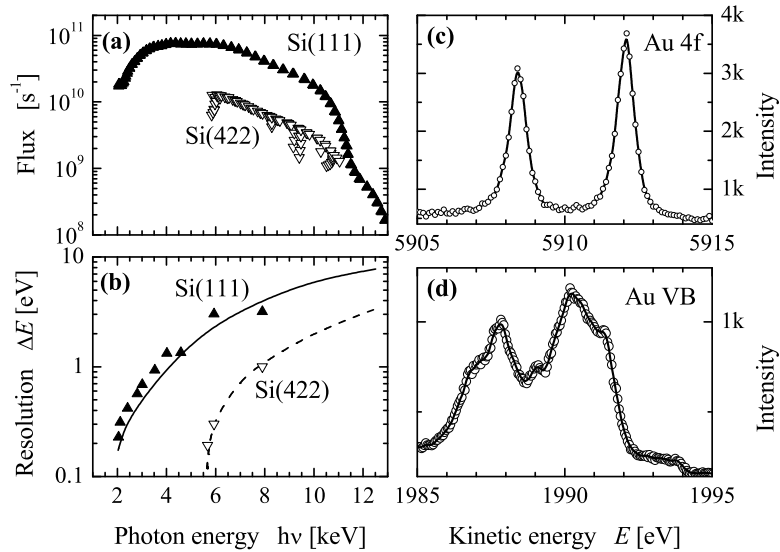


FIG. 1: Characteristics of the KM C-1 monochromator and the Phoibos 225 HV electron analyser. (a) shows the flux normalised to a current of 100 mA in the storage ring and (b) the calculated (lines) and measured (symbols) resolution of the monochromator. (c) and (d) show typical spectra of the Au 4f core level and valence band excited by 6 keV (Si(422)) and 2 keV (Si(111)) photons, respectively.

angle) and simultaneous spin-detection using a combination of a 2D-delay-line detector with a low energy Mott-detector. Typical spectra, as taken from a Au(100) single crystal are shown in Figure 1 (c) and (d).

Under the present experimental conditions an overall resolution of 240 meV at 2 keV photon energy has been reached (monochromator plus electron detector), as was determined from the Fermi edge of Au(100). Due to the low cross-section of the valence states from the investigated compounds, the spectra had to be taken with E_{pass} from 50 eV to 150 eV and a 1 mm entrance slit for a good signal to noise ratio. The polycrystalline CoTiSb samples have been cleaned in-situ by Ar⁺ ion bombardment before taking the spectra to remove the native oxide layer. Core-level spectra have been taken to check the cleanliness of the samples. No traces of impurities were found. All measurements have been taken at room temperature (≈ 300 K).

The self-consistent electronic structure calculations have been carried out using the scalar-relativistic full potential linearised augmented plane wave method (FLAPW) as provided by

Wien2k [14]. In the parametrisation of Perdew et al [15] the exchange-correlation functional was taken within the generalised gradient approximation (GGA). A $25 \times 25 \times 25$ mesh has been used for integration, resulting in 819 k-points in the irreducible wedge of the Brillouin zone. The properties of CoTiSb have been calculated in $F\bar{4}3m$ symmetry using the experimental lattice parameter ($a = 5.883 \text{ \AA}$) as determined by XRD. Co atoms are placed on 4a Wyckoff positions, Ti on 4c and Sb on 4d. This leaves the vacancy on the 4b position in accordance with the Rietveld refinement of the XRD data. All muffin-tin radii have been set as nearly touching spheres with $r_{MT} = 2.39a_{0B}$ for the 3d elements and $2.25a_{0B}$ for the main group element ($a_{0B} = 0.529177 \text{ \AA}$). A structural optimisation for the compound showed that the calculated lattice parameter deviates from the experimental one only marginally.

III. RESULTS AND DISCUSSION

Figures 2 (a) and (b) display the calculated band structure and density of states (DOS). The compound exhibits a clear gap in the band structure and DOS, that means it is semiconductor. The size of the gap amounts to about 1.45 eV. It is clearly visible that the gap is surrounded by regions of high density emerging from d-bands. The high density in the valence band emerges mainly from states located at the Co site, whereas the high density at the bottom of the conduction band is related to states located at the Ti site. The gap is a result of hybridisation with Sb states. The states at about 10 eV below the Fermi energy (E_F) are mainly located at the Sb site and have s-like character (see Fig. 3). This behaviour is typical for $C1_b$ compounds with overall 18 valence electrons in the unit cell.

The partial, atomic resolved (p) and the orbital (l) resolved densities of states are shown in Figure 3 (a) and (b), respectively. The p-DOS of the interstitial as well as the l-DOS for higher angular momenta (l) are omitted as they contribute only very few to the total density of states. The main contribution to states close to the Fermi energy are d-states being located at the Co site. As typical for $C1_b$ compounds with T_d symmetry, one finds a strong bonding interaction between transition metal d-states (t_{2g}) with Sb p-states (t_{1u}) that hybridise mainly along the $\Gamma-L$ direction [16]. This hybridisation leads here to the peak in the density at about 3 eV below E_F . The smaller peak at about -5 eV is due to s-p hybridisation.

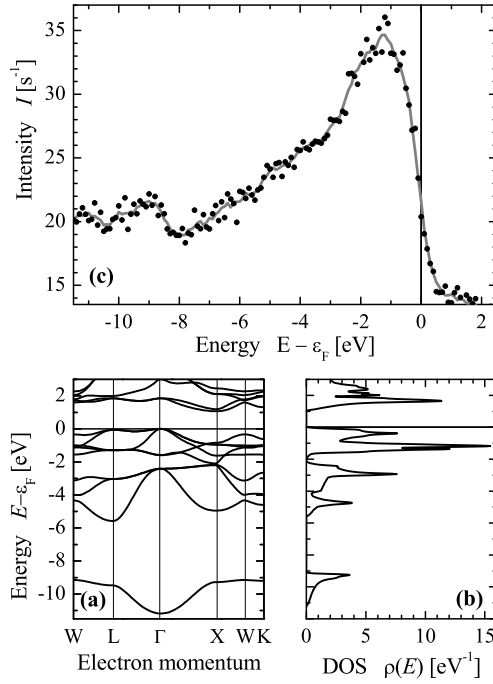


FIG. 2: XPS and density of states of CoTiSb.

Shown are the band structure (a) and the density of states (b) in comparison to a XPS spectrum excited by MgK radiation (c).

The valence band spectrum excited by MgK radiation is shown in Figure 2 (c). On a first sight, the spectrum exhibits a high intensity close to the Fermi energy and is rather unstructured at higher binding energies. The low lying s band at 9 eV to 11 eV below ϵ_F is only weakly revealed. Besides the maximum, there are only weak structures (compared to the calculated DOS) detectable in the energy region from -6 eV to ϵ_F . The maximum is located about 1.4 eV below ϵ_F and corresponds to the high density of Co d-states seen in the DOS.

The results from high energy photo emission are shown in Figure 4 and compared to the total density of states weighted by the partial cross sections. For better comparison, the weighted DOS is additionally broadened by a Gaussian of 0.25 eV (0.5 eV) width to account roughly for the experimental resolution at 2.5 keV (5 keV) excitation energy.

Both high energy spectra reveal clearly the low lying s-states at about -11 eV to -9 eV below the Fermi energy, in well agreement to the calculated DOS. The intensity in this energy region is considerably higher compared to the excitation at 1.2 keV (see Fig. 2). These low

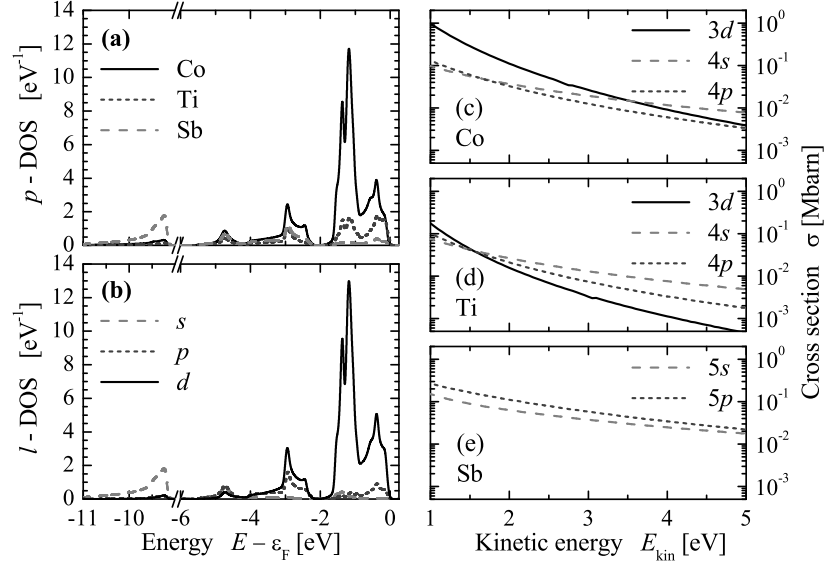


FIG. 3: Partial and orbital resolved densities of states and photo emission cross sections. Shown are the atomic resolved p-DOS in (a) and the orbital momentum resolved l-DOS in (b). (Note the axis break between -9 eV and -6 eV that was used to bridge the low lying hybridisation gap.) Panels (c)–(e) show the calculated energy and l dependence of the cross section of the valence states of atomic Co, Ti, and Sb.

lying bands are separated from the high lying d-states by the $C 1_b$ -typical hybridisation gap being clearly resolved in the spectra as well as the calculated DOS. The size of this gap amounts typically to $E \approx 3 \dots 4$ eV in Sb containing compounds.

Obviously, the emission from the low lying s-states is pronouncedly enhanced compared to the emission from the d-states. This can be explained by a different behaviour of the cross sections of the s, p, and d states with increasing kinetic energy as was recently demonstrated by Panaccione et al for the case of the silver valence band [8]. The orbital momentum and site resolved cross sections are displayed in Fig. 3 (c)–(e). The calculations were performed for atomic valence states using a modified full relativistic Dirac-solver based on the computer programs of Salvat and Mayol [17, 18]. The radial integrals for the various transitions have been computed using the dipole length-form. In particular, the cross section for d-states decreases faster with increasing photon energy than the ones of the s or p-states. This behaviour influences also the onset of the d-bands at about -7 eV to -6 eV. Just at the bottom

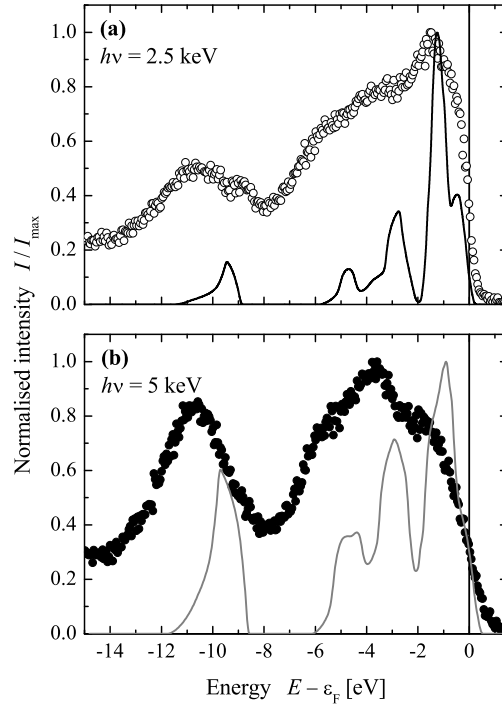


FIG. 4: High energy valence band spectra of CoTiSb.

Shown are spectra taken at 2.5 keV (a) and 5 keV (b) excitation energy (symbols) and the DOS weighted by the photo emission cross section (lines).

of those d-bands, they are hybridised with sp -like states, leading to a high intensity in this energy region. At $h\nu = 2.5$ keV, the structures of the weighted DOS have approximately the same heights compared to the DOS shown in Fig. 2 (b), whereas the strong enhancement of the s states is clearly visible if comparing Fig. 4 (a) and (b).

The structure of the high energy spectra in the range of the d states agrees roughly with the structures observed in the total DOS although the high density at -5 eV and -3 eV is not well resolved. Overall the emission from the d states covers a larger energy range compared to the calculated DOS, what gives advice on an underestimation of correlation effects in the local density approximation. However, one also has to account for lifetime broadening and the experimental resolution if comparing that energy range. At 2.5 keV excitation, the emission is still dominated by the high dense d -states at about -1.5 eV. Increasing the excitation energy to 5 keV (note the lower resolution of the monochromator at that energy) has the result that the intensity in this energy range becomes considerably lower. At the same time, the emission from the bands at about -3 eV becomes strongly enhanced. As

both structures in the DOS emerge, at least partially, from d -bands, the transfer of the intensity maximum might be not only explained by pure cross section effects.

The valence band spectra may be seen as a convolution of the initial and final state DOS. The final state DOS is rather constant at high kinetic energies and final state effects may play a minor role only. Two weighting factors enter the DOS-convolution. The first is the transition matrix element that contains both the selection rules and the cross sections (radial matrix elements). The radial matrix elements are partially responsible for the rearrangement of the orbital resolved intensities as discussed above. The second weighting factor is the complex self-energy of the photoelectron. Among other things, it depends on the hole lifetime. At low kinetic energies, the spectra are obviously governed by the long lifetime of the holes at binding energies close to E_F . At high kinetic energies, where the sudden approximation is reached, the photoelectron is not as strongly coupled to its hole and the lifetime at E_F plays less a role. Not only from the mean free path but also from the presented point of view, the high energy photo emission will help to understand the bulk electronic structure better than using only low energy XPS.

Overall, the measured photoelectron spectra agree with the calculated density of states. Small shifts of the peaks in the measured spectra compared to the calculated DOS give advice on an incomplete treatment of correlation effects in the local density approximation.

IV. SUMMARY AND CONCLUSIONS

The electronic structure of the ternary $C1_b$ compound $COTiSb$ was investigated by means of XPS. True bulk sensitive, high energy photo emission indicates that the cross section differs not only between states of different angular momentum but also depends on the binding energy for a fixed angular momentum. The first effect leads to a pronounced emission from low lying s bands. The second effect leads to a pronounced transfer of intensity away from the Fermi energy. It can be explained by a reduction of lifetime effects. Those lifetime effects govern the spectrum at low excitation energy and lead to an enhanced intensity close to the Fermi energy at low kinetic energies. Such lifetime effects can be reduced by use of high energy photo emission.

Acknowledgments

Financial support by the Deutsche Forschungsgemeinschaft (project TP 7 in research group FG 559) as well as by BESSY is gratefully acknowledged.

-
- [1] S. Tanuma, C. J. Powell, and D. R. Penn, *Surf. Interf. Anal.* 21, 165 (1993).
- [2] I. Lindau, P. Pianetta, S. Doniach, and W. E. Spicer, *Nature* 250, 214 (1974).
- [3] W. M. eisel, *Hyper ne Interact.* 45, 73 (1989).
- [4] K. Kobayashi, M. Yabashi, Y. Takata, T. Tokushima, S. Shin, K. Tam asaku, D. M iwa, T. Ishikawa, H. Nohira, T. Hattori, et al, *Appl. Phys. Lett.* 83, 1005 (2003).
- [5] A. Sekiyama and S. Suga, *J. Electron Spectrosc. Relat. Phenom.* 137–140, 681 (2004).
- [6] S. Thiess, C. Kunz, B. C. C. Cowie, T.-L. Lee, M. Reniera, and J. Zegenhagen, *Solid State Comm.* 132, 589 (2004).
- [7] K. Kobayashi, *Nucl. Instrum. Methods Phys. Res., Sect. A* 547, 98 (2005).
- [8] G. Panaccione, G. Causero, M. Causero, A. Fondacaro, M. Grioni, P. Lacovig, G. Monaco, F. O , G. Paolicelli, M. Sacchi, et al, *J. Phys.: Condens. Matter* 17, 2671 (2005).
- [9] P. Torelli, M. Sacchi, G. Causero, M. Causero, B. Krastanov, P. Lacovig, P. Pittana, R. Sergo, R. Tommasini, A. Fondacaro, et al, *Rev. Sci. Instrum.* 76, 023909 (2005).
- [10] R. A. de Groot, *Phys. Rev. Lett.* 50, 2024 (1983).
- [11] J. Tobola, J. Pierre, S. Kaprzyk, R. V. Skolozdra, and M. A. Kouacou, *J. Phys. Condens. Matter* 10, 1013 (1998).
- [12] B. Balke, K. Roth, G. H. Fecher, and C. Felser, *J. Magn. Magn. Mater.* xx, in print (2006).
- [13] Z. Kajsos, W. M eisel, P. Griesbach, and P. Gutlich, *Surf. Interface Anal.* 20, 544 (1993).
- [14] P. Blaha, K. Schwarz, G. K. H. Madsen, D. Kvasnicka, and J. Luitz, *WIEN2k, An Augmented Plane Wave + Local Orbitals Program for Calculating Crystal Properties* (Karlheinz Schwarz, Techn. Universitaet Wien, Wien, Austria, 2001).
- [15] J. P. Perdew, J. A. Chevary, S. H. Vosko, K. A. Jackson, M. R. Pederson, D. J. Singh, and C. Fiolhais, *Phys. Rev. B* 46, 6671 (1992).
- [16] D. Jung, H. J. Ko, and M. H. Whangbo, *J. Mol. Struct. THEOCHEM* 527, 113 (2000).
- [17] F. Salvat and R. Mayol, *Comp. Phys. Commun.* 62, 65 (1991).

[18] F. Salvat and R. Mayo, *Comp. Phys. Commun.* 74, 358 (1993).